Jordan Journal of Civil Engineering, Volume **13**, No. **2**, **2019**

Landslide Susceptibility Mapping Using Information Value Method

Virender Kumar Sarda [1] ***and Deepak Desh Pandey*** [2]

[1] Professor, National Institute of Technology, Hamirpur (HP), India.
E-Mail: sardavk@yahoo.com
[2] Research Associate, National Institute of Technology, Hamirpur (HP), India.
E-Mail: deepak2171985@gmail.com

ABSTRACT

The aim of this study is to utilize the remotely sensed data and GIS techniques for instability assessment of terrain and prediction in the chosen study area, Rohtang to Baralacha, Lahaul Spiti District, Himanchal Pradesh, India. Several parameter maps were generated by the availability of different types of multi-temporal and various scales of remote sensing data. Inventory map was developed though the field work, past records and with the help of remote sensing data. Geological map, soil map, land use map, terrain map, slope map, aspect map, drainage density and snow melt parameter maps were generated or extracted from the existing ancillary data. In speeding up processing for hazard zonation and prediction assessment, GIS can be useful. To determine the degree of susceptibility to the landslides, information value method is used. The landslide hazard map is classified on the basis of its probability values into low, medium, high and very high risk zones. The results showed that over 3.09% of the area is liable to low landslide risk, 26.28% of the area is liable to medium landslide risk, 32.81% of the area is of high landslide risk and within this area about 37.81% has very high to severe risk. The landslide susceptibility map delineated in this paper can be used by various stakeholders, like state governments, researchers and citizens to develop and manage the developmental activities in the area in particular and in other similar areas in general.

KEYWORDS: Landslide, Susceptibility map, Remote sensing, GIS, Information value method, Area under curve (AUC).

INTRODUCTION

Himalayan Mountains are tectonically active and associated with landslide activities (Sarkar et al., 1995; Rautela and Thakur, 1999; Anbalagan et al., 2008). Landslides are among the most common natural hazards in the LahaulSpiti district of Himachal Pardesh (India) and are responsible for large-scale transformations and massive destruction of life and property in the area. Lahaul is an ice-covered land mass and some of its most dramatic glaciers are Chota Shigri, Bara Shigri, Sona pani and Samundari glaciers (Chandel et al., 2011). Large-scale development activities, like hydro-power, tourism, transport networks, mining projects, among others, are leading to terrain alteration causing negative impacts on the environment of the Himalayas and resulting in landslides in many places. In order to decrease the threat of landslides, it becomes essential to develop a landslide susceptibility map. LHI is an important tool in distinguishing an area into a number of derived classes depending upon their susceptibility to landslide potential activities. Some major parameter characteristics, such as slope, aspect, relative relief, geological character, drainage and land use/land cover,

Received on 29/7/2017.
Accepted for Publication on 27/1/2019.

play an important role in deciding the potential vulnerable sites for slope failure. Several parameters and analytical approaches have been proposed along with different schemes for landslide hazard zonation using qualitative approaches or quantitative approaches (Carrara et al., 1977, 1978; Yin and Yan, 1988; Choubey and Litoria, 1990; Gupta and Joshi, 1990; Pachauri and Pant, 1992; Anbalagan and Singh, 1996; Soeters and van Westen, 1996; van Westen et al., 1997; Aleotti and Chowdhury, 1999; van Westen, 2000; Dai and Lee, 2002; Lin and Tung, 2003; Mathew et al., 2007; Sharma and Kumar, 2008; Pourghasemi et al., 2012; Sharbansarkar et al., 2013; Bibek Nepal et. al, 2015).

The present paper aims to generate information about the causative factors affecting landslides using remote sensing and other ancillary data and based on this to generate landslide hazard zonation maps using information value method. For this purpose, the study area has been selected in a part of Ravi river catchment along one of the landslide prone Chamba to Bharmour road corridor of NH-154A in Himachal Pradesh, India.The paper has been organized as follows: First, nature of the study area is presented ("study area" section). Then, research methods used in the study are discussed ("research methods" section). Then, sources from where data is collected are given along with the preparation of inventory map and maps of other causative factors selected in the present study in GIS platform ("data sources and data preparation" section). After this, results obtained based on the application of information value method for the preparation of landslide susceptibility map are validated and discussed ("results" section). Finally, the paper is concluded with the ("conclusion" section).

STUDY AREA

The area under investigation is located in between Rohtang and Baralacha la, Lahaul Spiti district and lies along NH-21 in the central zone of the Himalayas. Location of the area is between 77º14'47", 77º26' N latitudes and 32°22'17", 32º44' E longitudes and it possesses an intricate system of mountain ranges which is the result of successive compression movements of the Earth's crust (Burrard and Hayden, 1933). The total area of Lahaul and Spiti district is 13,617.91 Sq km and the study area covers 780.66 sq km surrounded by: in the north Pir-Panjal range; in the northwest Bara Bhangal; in the east Greater Himalayas; and in the southwest Dhauladhar range, while Sutlej River marks the southern boundary of the district (Figure 1). This district has a very high absolute relief ranging from 2344 to 6320 meters. The geomorphological character of Lahaul is influenced by both glacial and fluvial processes and the area is generally separated into glaciers, permanent snowfields, rocky/barren slopes, valley slopes, ridges and main valley floor (Sah and Mazari, 2007). In most of the eastern parts of the study area at the altitude of 6320 meters, glaciers and permanent snow fields are found. The lower parts of glaciers and permanent snow fields are occupied by barren/rocky valley slopes and these valleys are separated into steep to moderately steep slopes, ridges and narrow valleys, where slopes usually have an inclination of 10º to 81º. Outwash fans, alluvial fans and river terraces are the main geomorphological characteristics of the Chenab River, which conquered the valley of the study area. The total population of the district is 31,528 persons with population density being 2 persons per km² (2011 census). Tourism industry plays a major role in the development of Lahaul district.

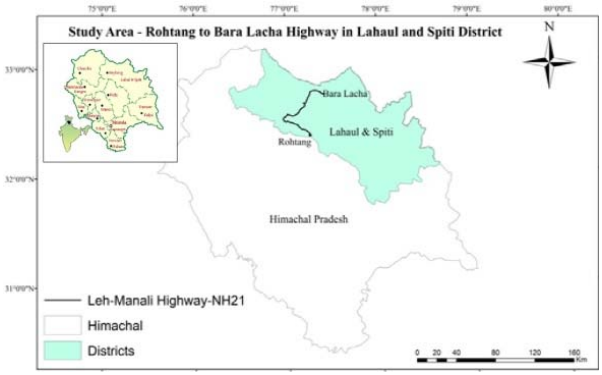

Figure (1): Study area (Rohtang to Baralacha la)

RESEARCH METHODS

Two steps are involved in the present study: (i) preparation of landslide inventory map and (ii) application of bivariate statistical method for developing the landslide susceptibility map of the study area.

Landslide Inventory Map

Landslide inventory maps are prepared for multiple reasons, like: (i) documenting the extent of landslide phenomena in areas ranging from small to large watersheds (Cardinali et al., 2001) and to large regions both at national and global levels (Trigilia et al., 2010), (ii) as a preliminary step towards landslide susceptibility, hazard and risk assessment (Balteanu et al., 2010), (iii) for investigating the distribution, types and patterns of landslides in relation to characteristics, like morphological and geological charateristics,… etc. (Guzzetti et al., 1996) and (iv) to study the evolution of landscapes dominated by mass-wasting processes (Parker et al., 2011). In general, it is a landslide database that records the location, date of occurrence (where known), landslide type, parameters and properties (Guzetti et al., 2012). Landslide inventory maps can be prepared using different techniques depending on the purpose of the inventory, extent of study area, scale of base maps, scale, resolution and characteristics of available imagery and skills and experience of investigators (van Westen et al., 2006).

Bivariate Statistical Analysis

Based on the assumption that the factors controlling the occurrence of landslides in a region in the past are the same as those that will cause landslides in the future, bivariate statistical analysis compares each data layer of causative factors to the existing landslide distribution; i.e., location. Based on landslide density, weights are assigned to the causative factors. Various bivariate statitstical methods used in landslide hazard zoanation mapping are: frequency analysis approach, information value model (IVM), weights of evidence (WOE) model, weighted overlay model,… etc. In the present study, we used the information value model which has already been proved to be a useful method in determining the degree of influence of individual causative factors responsible for landslide occurrence (Arora et al., 2004; Champatiray et al., 2007; Kanungo et al., 2009).

The information value model which is a statistical analysis method proposed by Yin and Yan (1988) and modified by van Westen (1993) was first used in the prospecting field and was later applied to spatial prediction of geological hazards and disaster risk assessment. In this method, the weighted class value is determined based on the density of landslides in each causative parameter (Lin and Tung, 2003).

A landslide $L$is caused by many factors, like geology, structure, slope gradient, slope aspect, altitude, rainfall,… etc. This method aims to find the probability of a landslide event based on the comprehensive information available of the significant factors. The information value is defined as:

$$I(\mathrm{L},\mathrm{x}_1,\mathrm{x}_2,\mathrm{x}_3,\ldots\mathrm{x}_n)=\ln\frac{P(\mathrm{L},\mathrm{x}_1,\mathrm{x}_2,\mathrm{x}_3,\ldots\mathrm{x}_n)}{P(L)} \quad (1)$$

where $I(\mathrm{L},\mathrm{x}_1,\mathrm{x}_2,\mathrm{x}_3,\ldots\mathrm{x}_n)$ is the information value of a landslide provided by a specific combination of factors $x_1,\mathrm{x}_2,\mathrm{x}_3,\ldots\mathrm{x}_n$,$P(\mathrm{L},\mathrm{x}_1,\mathrm{x}_2,\mathrm{x}_3,\ldots\mathrm{x}_n)$ is the probability of a landslide under the combination of factors $x_1,\mathrm{x}_2,\mathrm{x}_3,\ldots\mathrm{x}_n$,$P(L)$ is the probability of a landslide. Based on the computation of the conditional probability, Eq. 1 can be written as:

$$P(\mathrm{L},\mathrm{x}_1,\mathrm{x}_2,\mathrm{x}_3,\ldots\mathrm{x}_n)=I(\mathrm{L},\mathrm{x}_1)+ I_{x_1}(\mathrm{L},\mathrm{x}_2)+\ldots\ldots\ldots+I_{x_1x_2x_3\ldots\ldots x_{n-1}}(\mathrm{L},\mathrm{x}_n) \quad (2)$$

where $I_{x_1}(\mathrm{L},\mathrm{x}_2)$ is the information value of a landslide provided by factor x_2 when factor x_1 exists. It is clear from Eq. 2 that the information value of a landslide provided by the combination of factors $x_1,\mathrm{x}_2,\mathrm{x}_3,\ldots\mathrm{x}_n$is equal to the sum of the information value provided by factor x_1 and the information value of a landslide provided by factor x_2 when x_1 is determined and the information value of a landslide provided by factor x_n when $x_1,\mathrm{x}_2,\mathrm{x}_3,\ldots\mathrm{x}_{n-1}$ are determined. However, in the practical application, the information value of each factor can be calculated from:

$$I(L,x_i) = \ln \frac{\frac{Npix(Si)}{Npix(Ni)}}{\frac{\sum \text{Npix (Si)}}{\sum \text{Npis (Ni)}}} \quad (3)$$

where $I(L,x_i)$ is the information value of a factor class; $Npix\,(Si)$ is the number of pixels of a landslide within class i; $Npix\,(Ni)$ is the number of pixels within class i; $\sum Npix(Si)$ is the number of pixels of a landslide within the entire study area; $\sum Npix\,(Ni)$ is the number of pixels within the entire study area.The landslide susceptibility index (LSI) for each pixel was computed by summing the information values of each factor class as follows:

$$LSI = \sum_{i=1}^{n} I(L.x_i) = \sum_{i=1}^{n} In\ \frac{\frac{Npix(Si)}{Npix(Ni)}}{\frac{\sum \text{Npix (Si)}}{\sum \text{Npis (Ni)}}} \quad (4)$$

It should be noted that when $LSI < 0$, the likelihood of a landslide is less than average; when $LSI = 0$, the likelihood of a landslide is equal to average; when $LSI > 0$, the likelihood of a landslide is greater than average. This indicates that the greater the information value, the greater the possibility of a landslide.

DATA SOURCE AND DATA PREPARATION

Data Soure

The analysis of the study area is carried out on the basis of Survey of India, Geological Survey of India and satellite imagery (Table 1). Google Earth images of the year 2015 and GPS measurements which were taken from the field work of the study area were used to develop an inventory of the landslides which occurred in the past. Various th ematic maps, like: slope, aspect, relative relief, drainage, geological structure and land use/land cover maps are generated with the help of Arc GIS 10.1 and ERDAS 9.3 software and slope, aspect and relative relief layers were derived from the Cartosat DEM and '3D Analyst' tools in Arc GIS 10.1, while drainage density analysis was performed using 'Hydrology' tools and 'Fishnet' analysis in ArcGIS10.1. In order to derive a meaningful land use/land cover classification map from satellite imagery (LISS III, 1D), NDVI analysis was applied.

Table 1. Data type/source for landslide hazard zonation

Sr. no.	Data type	Data description	Use/ purpose
1	Topographical Sheet Scale	1:50,000	DEM: Slope, Aspect, Relative Relief, Drainage Network and Density
	Satellite Data Cartosat DEM	Spatial Resolution 1m	
2	IRS-P6 LISS III	Spatial Resolution 23.5m	Land use/land cover
3	Geological Map	Scale 1:50,000	Geology, Lithology
4	Soil Map	Scale 1:50,000	Soil
5	Field Data	GPS Locations	Landslide locations

Data Preparation

1. Landslide Inventory Map

Distribution analysis is the simplest qualitative LHZ mapping approach. It is also known as 'landslide inventory'. This analysis is carried out on the basis of spatial and temporal patterns of landslide distribution, type of movement, rate of movement, type of displaced material (earth, debris or rocks,… etc.) by which landslide inventory maps are produced (Figure 2). This data is obtained through field survey mapping, historical records, satellite images and Google Earth 2013 images. Cruden (1991) defined landslide inventory as 'the simplest form of landslide information which records when and where the landslide occured and the type of landslides that have left identifiable traces in the area'.

The landslide inventory map also shows a slope failure by a single event or may show the cumulative effect of many events (Guzzetti et al., 2006). Landslide inventory plays a significant role in landslide hazard assessment. Landslide inventory, distribution, geomorphological maps of landslides and multi-temporal landslide inventories have been compiled and the relationships among them were established. The results of the study showed that a complete landslide inventory map provides high predictive power for landslide susceptibility analysis.

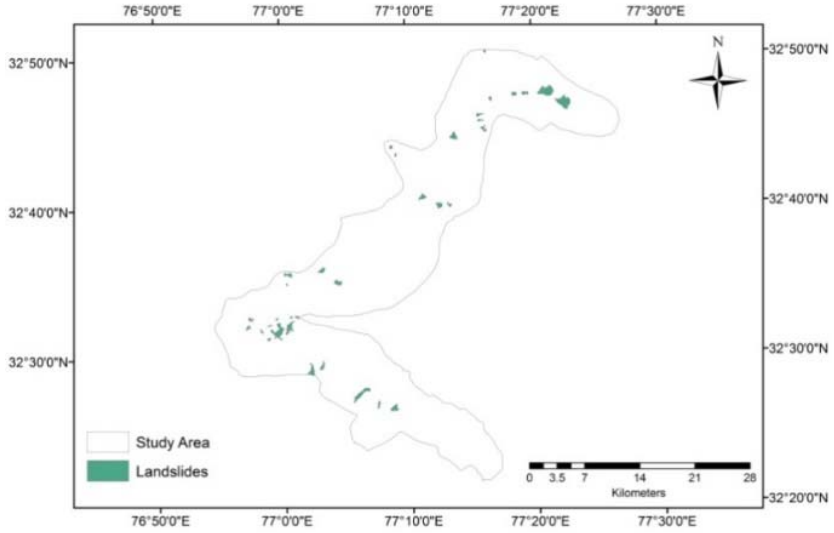

Figure (2): Landslide inventory map

2. Landslide Causative Parameters

The selection of parameters causing landslide depends on various factore, like the nature of the study area, landslide type, failure mechanism, scale of analysis and *a priori* knowledge of the main causes of landslides (Jaiswal, 2011). However, these selected parameters must also be operational, measurable, well representing the whole study area and should vary spatially (Yalcin, 2008).

In the present study, about 8 parameters have been selected for the susceptibility analysis based on field observations, landslide characteristics and information from previous studies and reports.

(i) Slope and Aspect

Slope and aspect are both important triggering factors that determine the hazards of an area. The slope degree is defined as the rate of change in elevation over distance (Figure 3). The lower slope values represent less steep terrain and the higher values represent steeper terrain. The slope can be determined from (Chandel et al., 2011):

$$\text{Slope (degree)} = 57.3 \tan^{-1} \sqrt{\left(\frac{dz}{dx}\right)^2 + \left(\frac{dz}{dy}\right)^2} \qquad (5)$$

The study area has gentle slopes ranging from nearly 10º to 81º from Rohtang to Baralacha la and such slopes are found either along the river's course or on ridge tops. The slope map is divided into five classes (normal slope 0º - 10º, moderate slope 11º- 25º, steep slope 26º - 38º, very steep slope 39º - 51º and extremely steep slope 52º-81).

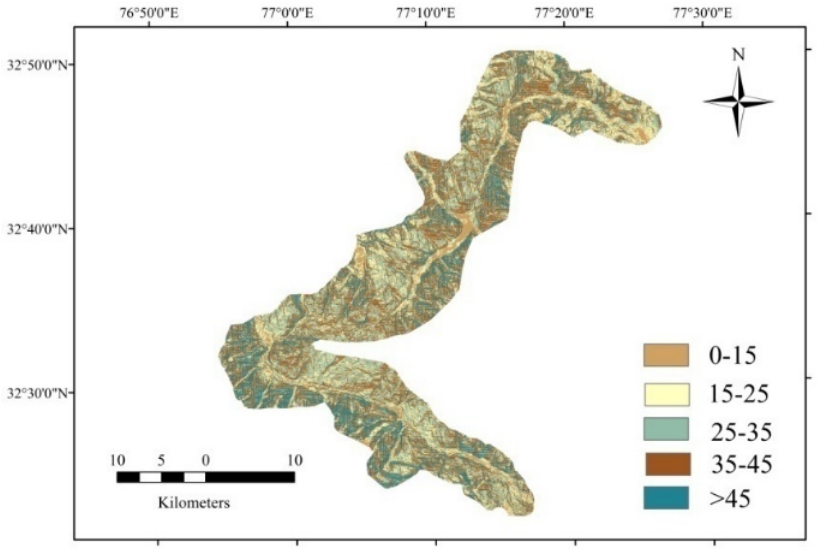

Figure (3): Slope map

Aspect defines the down slope direction of the maximum rate of change or the direction of steepest slope in x-y plane. Aspect can be determined from Chandel et al. (2011):

$$\text{Aspect} = 57.3A\ tan^{-1}\ 2\left[\left(\frac{dz}{dy}\right) + \left(\frac{dz}{dx}\right)\right] \quad (6)$$

In Eq. 5 and Eq. 6, dz/dx is the rate of change in $x-$direction and dz/dy is the rate of change in $y-$direction.

The aspect distribution along NH -21 from Rohtang to Baralacha la is even in all eight directions (Figure 4). The aspect is significant for understanding the slope stability. Usually, southeast (SE) to south (S) and southwest (SW) slopes are comparatively more prone to the failure of slope and sliding activities.

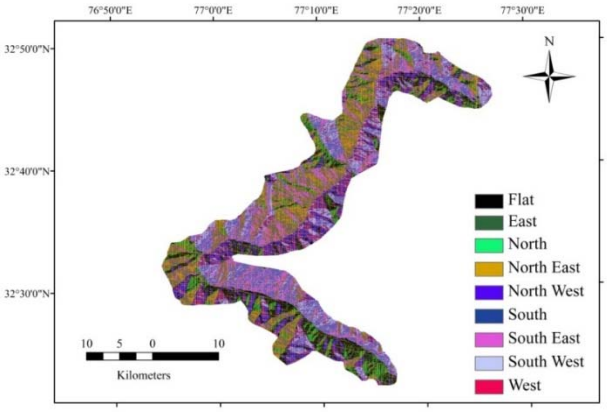

Figure (4): Aspect map

(ii) Physiography and Relief

In the study area, high relief and local relief are calculated from the difference between the highest and the lowest altitude. Rapid rise in altitude, as well as

presence of faults are found in the high-relief region, while mature topography signifies lower relief. Most important triggering factors for landslide are morphological character and relative relief of an area. Relative relief plays an important role in the vulnerability of settlements, transport network and land as a risk agent. In the study area, there is a wide variation in relative relief (Figure 5) ranging from low to high which is classified into three classes: low (below 2851m), moderate (2852-5941m) and high (above 5942m) relative relief, respectively.

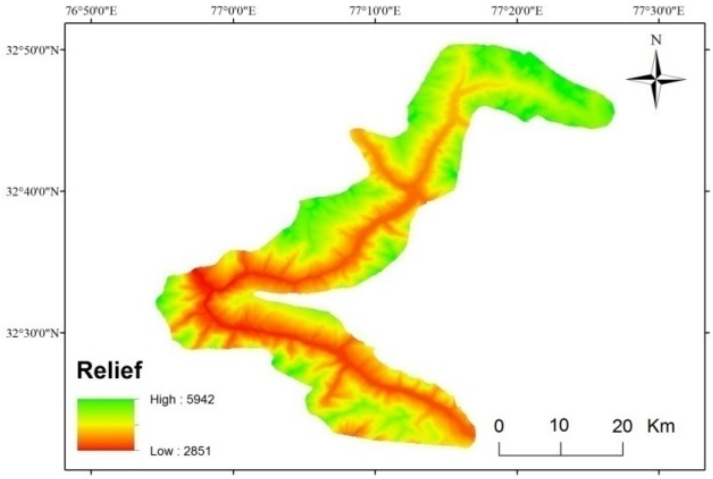

Figure (5): Physiographic and relief map

(iii) Geological Structure

Rocks of the study area in the Lahaul district along NH -21 are from the Proterozoic era to the quaternary period in accordance with the geological time scale. In the Lahaul group, the major litho-tectonic unit expresses the geology of the area. The area is dissected by several major thrusts, Lahaul thrust and Vaikrita thrust (which are still active) along with the several local faults/lineaments. These thrusts play a major role in the neo-tectonics of the area (Choubey et al., 2007). The Jutogh thrust separates rocks belonging to Lahaul group and Jutogh group, while Lahaul thrust or Chail thrust (Bhargava and Bassi, 1994) defines boundary between the rocks of the Rampur Larji group and the Lahaul group. Structurally, the main Lahaul valley is a synclinorium/ gently folded antiform having river Beas following its axial plane along the fault running in the NNW-SSE direction from the upper catchment, where it is intersected by a cross-fault almost at right angles (Sah and Mazari, 2007). This fault is a dextral tear fault with a dislocation of nearly 1.5 km (Shankar and Dua, 1978). In the study area, alluvium/ sandstone and quartzite, assorted material, limestone/granitoid genesis, moraine complex/phyllite, quartzite, sandstone/ flood plain, shales, snow/ shist are found. Phyllite and schist are the most fragile rocks, in which a number of faults and joints were found (Figure 6).

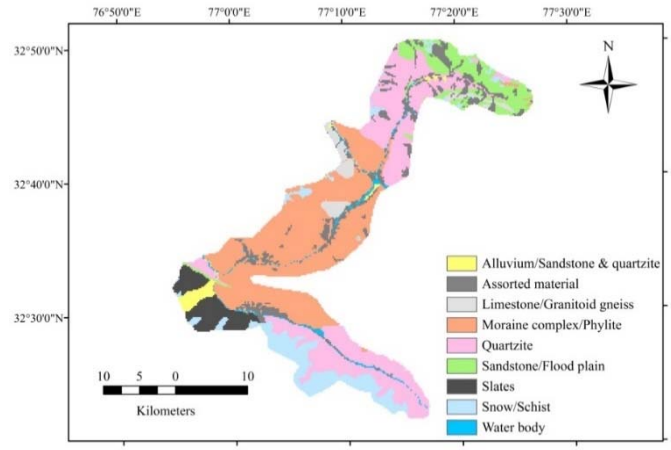

Figure (6): Geological map

(iv) Soil

In the study area, mesic loamy-skeletal stony soils, calcareous coarse loamy soils with slight erosion, well drained loamy soils with moderate erosion and snow-covered outcrops are found (Figure 7). These soils play an important role in the debris flow movement. This map was generated with the help of Himanchal Pradesh soil map collected from the Survey of India (SOI).

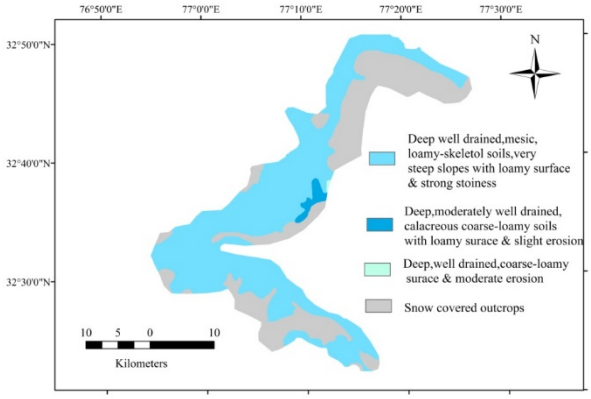

Figure (7): Soil map

(v) Drainage Character

Drainage patterns are an outcome of the long-time interaction between the geological structure, topography and slope. In the study area, the early stage of drainage network shows a dendritic pattern. A mathematical expression of drainage morphometry of an area is the drainage density (Eq. 7), which is a measure of the length of stream channel per unit area of drainage basin (Figure 8).

$$Drainage\ density, D_d = \frac{Stream\ length\ (L)}{Basin\ area\ (A)} = \frac{\sum_{1}^{n} L}{A} \qquad (7)$$

The drainage density is useful in the measurement of landscape dissection and runoff potential. Higher degree of dissection of land indicates higher probability of slope failure. Drainage density in the study area (Figure 8) has been divided into: low, medium and high. The low-density area mostly comprises of mountain tops, major ranges and ridges. The valley floors of all the major streams have high drainage density. Such areas account for only 8% of the total area of the district.

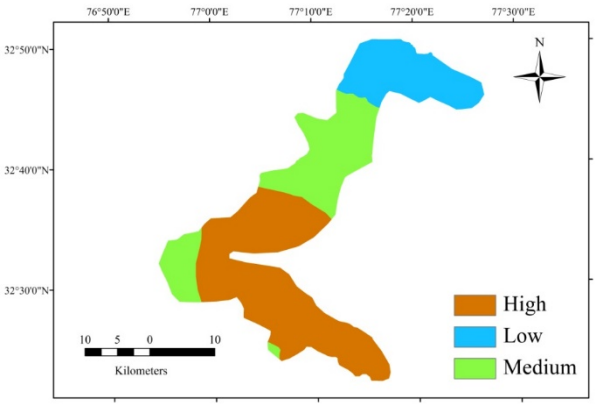

Figure (8): Drainage density

(vi) Land use/land cover

Relationships between land use, disaster risk and vulnerability to disaster events reflect the land use /land cover analysis. The land use/ land cover analysis is based upon LANDSAT ETM+ (2000) and (2005), IRS-P6 LISS-III 1D and Cartosat DEM. The land use classification of mountainous terrains suffers from certain drawbacks, such as high relief resulting in shadow areas and confusion between land use classes, like areas covered with barren, rocky surfaces, water bodies, forests, glaciers, dense snow and melted snow (Figure 9). Normalized Difference Vegetation Index (NDVI) was calculated to reduce the error in classification, which helps in enhancing the spectral difference between different objects using the formula:

$$NDVI = \frac{(NIR-R)}{(NIR+R)} \quad (8)$$

Here, NIR represents the spectral reflectance of objects in the near infrared band, while R represents the same in the red band. In addition, the cartosat digital elevation model (DEM) was used to eliminate the possibility of land use classes which are being wrongly categorized by adding some criteria. In the present study, maximum likelihood classification (MLC) algorithm which is the most accurate classifier (Foody et al., 1992; Richards and Jia, 1999; Saha et al., 2005) has been used.

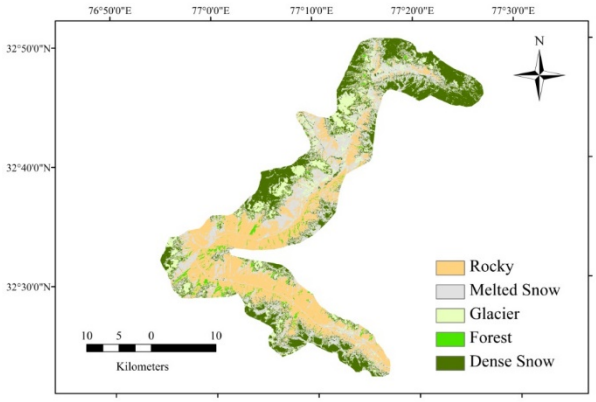

Figure (9): Land use/land cover map

(vii) Snow melt

Relationships between land cover and snow melt to disaster events reflect the snow melt analysis. In the study area, satellite imageries LISS-III-1D (23.5 m resolution) of January 2013 and July 2013 were used to prepare the snow melt map (Figure 10). Analysis is based upon change detection mapping. Land cover classification of these images shows a dense snow area. The high mountainous terrains suffer from certain drawbacks, such as high relief resulting in shadow areas and confusion between land use classes like barren rocky hills, melted snow, dense snow, glaciers and forests. Snowmelt was calculated with the help of a detection tool in GIS.

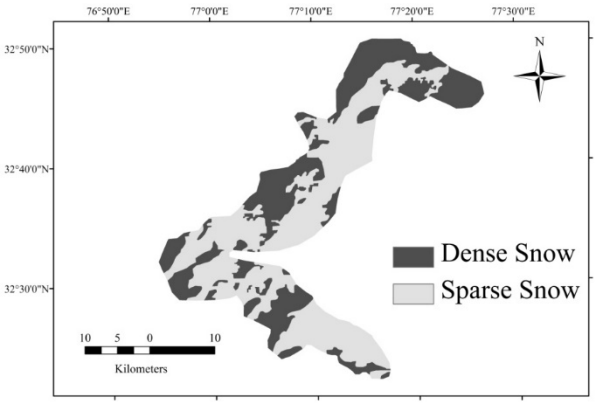

Figure (10): Snow melt map

RESULTS

Landslide Parameter Class Weight

Table 2 shows the relationship between landslide distribution and landslide controlling factors. The relationship is reflected by the weight values of the parameter classes. Negative weight value of any parameter class means that its presence may not contribute to the occurrence of landslides. On the other hand, a positive weight value means that the particular parameter class characteristics or occurrence may enhance the probability of landslides. A weight value around zero (±0.1) indicates neither the presence nor the absence of landslides (van Westen et al., 2003).

Magliulo et al. (2008) demonstrated that consideration of landslide detachment zones rather than landslide body for statistical analysis conveys a meaningful result of the susceptibility assessment. Therefore, in the present study, only the area of landslide detachment zones was used for statistical analysis.

Table 2. Information value table

Class	Class-Name	Count	Total no. of pixels in landslide	Con.Prob.	Prior Prob.	Con. Prob./ Prior Prob.	Information Value
Slope	0-15	273454	7910	0.0289	0.3864	0.0749	-1.1257
	15-25	245956	30361	0.1234	0.3864	0.3195	-0.4955
	25-35	309779	244194	0.7883	0.3864	2.0403	0.3097
	35-45	314654	198691	0.6315	0.3864	1.6344	0.2134
	>45	211605	42534	0.2010	0.3864	0.5203	-0.2838
Aspect	Flat	271829	0	0	0.3864	0	0
	North	91204	54860	0.6015	0.3864	1.5569	0.1923
	Northwest	94666	111897	1.1820	0.3864	3.0594	0.4856
	West	89049	124993	1.4036	0.3864	3.6330	0.5603
	Northeast	202997	46381	0.2285	0.3864	0.5914	-0.2281
	Southwest	190358	48323	0.2539	0.3864	0.6570	-0.1824
	East	108264	53403	0.4933	0.3864	1.2767	0.1061
	Southeast	198903	35335	0.1776	0.3864	0.4598	-0.3374
	South	108178	48498	0.4483	0.3864	1.1604	0.0646
LULC	Forest	30982	5687	0.1836	0.3864	0.4751	-0.3232
	Rocky	390836	186371	0.4769	0.3864	1.2342	0.0914
	Dense snow	382582	105443	0.2756	0.3864	0.7133	-0.1467
	Glacier	169947	104919	0.6174	0.3864	1.5979	0.2035
	Melted snow	381101	121270	0.3182	0.3864	0.8236	-0.0843
Lithology	Assorted material	150232	111636	0.7431	0.3864	1.9233	0.2841
	Quartzite	153449	76094	0.4959	0.3864	1.2835	0.1084
	Slates	149531	52176	0.3489	0.3864	0.9031	-0.0443
	Alluvium/sandstone and quartzite	148850	51491	0.3459	0.3864	0.8953	-0.0480
	Limestone/granitoid gneiss	149132	51777	0.3472	0.3864	0.8986	-0.0464
	Water body	148841	0	0	0.3864	0	0
	Sandstone/flood plain	149977	51195	0.3414	0.3864	0.8835	-0.0538
	Moraine complex/phylite	155080	78140	0.5039	0.3864	1.3041	0.1153
	Snow/schist	150356	51181	0.3404	0.3864	0.8810	-0.0550

Soil	Deep well-drained, mesic, loamy-skeletal soils, very steep slopes with loamy surface and strong stoniness	345596	295618	0.8554	0.3864	2.2140	0.3452
	Snow-covered outcrops	340706	111839	0.3283	0.3864	0.8496	-0.0708
	Deep, well-drained, coarse-loamy surface and moderate erosion	334434	27579	0.0825	0.3864	0.2134	-0.6707
	Deep, moderately well-drained, calacreous coarse-loamy soils with loamy surface and slight erosion	334712	57306	0.1712	0.3864	0.4431	-0.3535
Drainage Density	Low	449382	89696	0.1996	0.3864	0.5166	-0.2868
	Medium	450993	108802	0.2412	0.3864	0.6244	-0.2045
	High	455073	325192	0.7146	0.3864	1.8496	0.2671
Snow Melt	Dense snow	675827	104287	0.1543	0.3864	0.3994	-0.3986
	Sparse snow	679621	419403	0.6171	0.3864	1.5973	0.2034

Landslide Susceptibility Map

Finally, all the thematic layers are converted into 20m x 20m grid cells; then, the relation between the causing factors and the existing landslides was analyzed. Subsequently, the contribution of each class in the factors for landslide occurrence is calculated. To prepare the landslide susceptibility map, the weight value for each class of the causative factors was calculated (Table 2) and landslide susceptibility index (LHI) for each pixel was computed by summing up the weighted values of each factor class. The index values were classified into four susceptibility classes; i.e., very high, high, moderate and low. The classification was done automatically in ArcGIS. The final LSM prepared is shown in Figure 11.

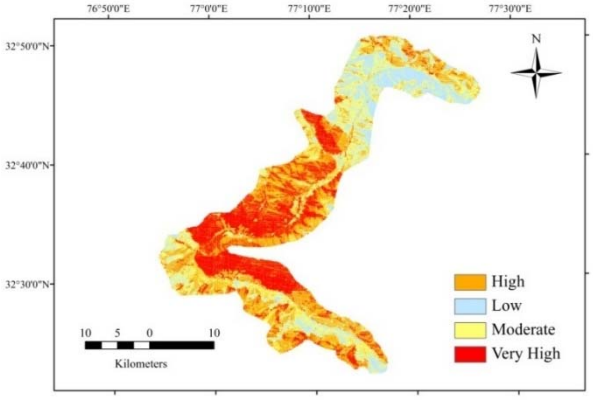

Figure (11): Landslide susceptibility map

It has been noted that out of the total area of 780.66km^2 under study, about 3.1% area falls under low-susceptibility zone, 26.3% falls under medium-susceptibility zone, 32.8% falls under high-susceptibility zone and 37.8% falls under very high-susceptibility zone.

Validation of Landslide Susceptibility Map

Validation of LSM derived is essential to ascertain the applicability of the method used for practical purposes (Chung and Fabbri, 2003). Several methods (Chung and Fabbri, 2003; Guzetti et al., 2006; Frattini et al., 2010) are available in the literature to validate the quality of susceptibility map. In the present study, ROC curve method has been used to validate the results of LSM. In this method, area under the curve (AUC) values are the basis of accuracy assessment of the model. The AUC leads to determine the quality of the probabilistic model by describing its ability to reliably predict the occurrence or non-occurrence of landslide events (Fawcett, 2006; Nandi and Shakoor, 2009; Feizizadeh et al., 2013). The ROC curve has been developed by extracting true positive (sensitivity) and false positive (1-specificity) rates from the contingency tables associated with different cutoff values for each model, using the following formulae (Zweig and Campbell, 1993). The ROC curve has been obtained by plotting true positive rate against false positive rate as shown in Figure 12. On the plot, marked is also the probability of occurrence of debris landslide.

The range of values of the ROC area should be within (0.5-1) for a good fit, while values below 0.5 represent a random fit. From Figure 12, the area under curve (AUC) comes out to be 0.832, which can be considered as excellent (Hosmer and Lameshow, 2000) and indicats that the overall success rate is about 83.2%. Hence, the generated map has exhibited promising results.

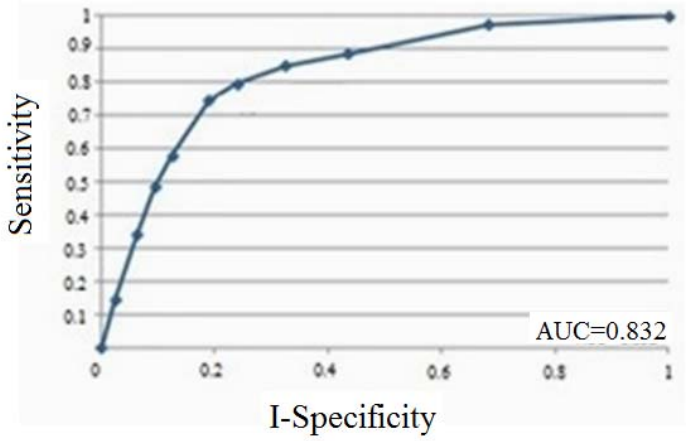

Figure (12): ROC curve for validating debris landslide susceptibility map

DISCUSSION

Whether a delineated landslide susceptibility map is of high quality or not relies upon the nature of the information parameters which are chosen in an investigation. Landslide inventory data is the primary parameter. In the present study, landslide inventory has been prepared utilizing satellite imageries, field work and limited historical records. It is pointed out here that exclusive those landslides having known location and

type were utilized in the analysis. Fundamentally, the landslides recorded are along the roads and cut-slope area, which prompts spatial bias of the landslide incidents. It can be noticed that in the investigation zone, every one of the sub-classes has a weight equal to or greater than zero, demonstrating that all parameters bring about the likelihood of landslide occurrence, yet to different extents. It can be noted from Table 2 that the largest weights correspond to slope of 25º -35º covering about 46.6% of landslides, followed by slopes of 35º-45º having around 37.9% of landslides. For other slope classes, the likelihood of occurrence of landslides was significantly less. It can be noticed that around 84.6% of the landslides occurred in the slope range between 25° and 45°.

Among the slope-aspect categories, the most extreme weight was found on the west-bound slope (0.56) and the least on the south-east faces (-0.33). In this way, most extreme quantities of landslides were concentrated in the west and the north-west slope direction in contrast to others. This can be attributed to the rainfall distribution patterns with rain brought by the south-eastern storms. In light of the LULC, landslides generally happened within the glacier areas with the highest rating (0.20), followed by rocky hills (0.09), dense snow (-0.1), melted snow (-0.08) and forests (-0.32). This is justifiable, as the area is extremely influenced by snowfall during winters. Among the lithological classes, land with snow/schist has a low contribution to landslide occurrences and the majority of landslides occurred in moraine complex/ phyllite (0.12), followed by assorted material (0.28), limestone/granitoid gneiss (-0.05), quartzite (0.11), slates (-0.04), sandstone/flood plain (-0.053) and alluvium/sandstone and quartzite (0.05). This indicates that the study area is dominated by moraine /phyllite soil. The weight value of the quartzite and quaternary sediment class suggests that it does not contribute much to the presence of landslides.

For the most part, deep well-drained, mesic loamy, skeletal soils, very steep slopes with loamy skeletal soils, very steep slopes with loamy surface and strong stoniness contributed much to the landslide occurrences (0.35), followed by snow-covered soils (-0.06), deep, well-drained, coarse loamy surface with moderate erosion surface (-0.21) and by deep, moderately well-drained, calcareous coarse-loamy soils with loamy surface and slight erosion (-0.35). In view of the drainage density, most slope failures (62.06%) occurred inside the high-drainage density zone with a weight value of (0.26), followed by medium-drainage density zone (20.78%) and low-drainage density (17.13%). The impact of snow melt can be isolated into two zones, which shows that high-slope failures (80.09%) happened in the sparse snow-covered zone and less-slope failures (19.91%) in the dense snow-covered zone.

Although some of the landslide factors and landslide incidence relationships are inconsequential, the outcomes can be utilized to comprehend their contributions based on their factual condition and occurrence in the field. For instance, the river distance and density factor map delineates insignificant contribution to the landslide events. This can possibly be due to the abundance of trees thriving along the river banks, which impeded slope erosion and landslides.

CONCLUSIONS

The present study focused on the qualitative analysis of landslides along NH-21, from Rohtang to Baralacha la in Lahaul-Spiti district of Himachal Pradesh in India. GIS and information value have been used for the landslide susceptibility. A total of seven factor maps of slope, aspect, geology, soil, land use /cover, drainage density and snow melt were generated using GIS software. Standardization of the causative factors has been done in detail by using the information value method, in which weights were calculated for each factor. The weights of factors influence the results of landslide susceptibility assessment. The weighted rating approach was used in the arithmetic overlay analysis in GIS. The numerical data layers representing the weight values of the factor classes as an attribute information were generated from the thematic data layers for the

purpose of data integration and spatial analysis in GIS. Within thirty nine categories belonging to seven causative factors, geology of the area that contains moraine complex, phyllite, slates, sandstone and alluvium, slopes between 25° and 45°, south and south-east aspect, loamy skeletal soil cover, high drainage density and dense snow cover were the main factors responsible for landslides. Based on the total weight, the debris landslide susceptibility map was generated in GIS. The study area has about 37.8% of its area under very high susceptible zone, 32.8% under high susceptible zone, 26.3% under medium susceptible zone and only 3.1% under low susceptible zone, as shown in Figure 12. The susceptibility map results have been validated with the Receiver Operating Characteristics (ROCs) curve. Results after validation give the area under curve [AUC] value as 0.832, which shows 83.2 % accuracy, indicating that the produced map has exhibited promising results.

ACKNOWLEDGEMENT

This paper is a part of the Department of Science and Technology, Ministry of Science and Technology, Government of India sponsored project "GIS-based Snow Melt Water/Rainfall Induced Debris Flow Landslide Susceptibility Assessment between Rohtang and Baralacha la in Himachal Pradesh, India". Authors duly acknowledge the support of DST for carrying out this project at National Institute of Technology, Hamirpur (HP). Authors are thankful to Dr. Bhoop Singh and Dr. A. K. Singh of Department of Science and Technology, Ministry of Science and Technology, for their valuable suggestions from time to time.

REFERENCES

Aleotti, P., and Chowdhury, R. (1999). "Landslide hazard assessment: summary review and new perspectives". Bulletin of Engineering Geology and the Environment, 58 (1), 21-44.

Anabalagan, R., and Singh, B. (1996). "Landslide hazard and risk assessment mapping of mountainous terrains- a case study from Kumaun Himalaya, India". Engineering Geology, 43, 237-246.

Anabalagan, R., Chakraborty, D., and Kohli, A. (2008). "Landslide hazard zonation (LHZ) mapping on meso-scale for systematic planning in mountainous terrain". Jounral of Scientific and Industrial Research, 67, 486-497.

Bălteanu, D., Chendeş, V., Sima, M., and Enciu, P. (2010). "A country-wide spatial assessment of landslide susceptibility in Romania". Geomorphology, 124, 102-112.

Bibek Nepal, P., Jagadeeswara Rao, and Tran van Ho. (2015). "Geographical information system-based landslide susceptibility index mapping using information value method - a case study of Sindhuplachok district, Nepal". International Workshop on Role of Land Professionals and SDI in Disaster Risk Reduction. In context of POSL 2015 Nepal Earthquake, FIG-ISPRS Workshop. Kathmandu, Nepal, November 25-27, 1/15-15/15.

Cardinali, M., Antonini, G., Reichenbach, P., and Guzzetti, F. (2001). "Photo-geological and landslide inventory map for the Upper Tiber River basin". CNR, Gruppo Nazionale per la Difesadalle Catastrofi Idrogeologiche, Publication n. 2116, Scale 1:100,000.

Carrara, A., Catalano, E., Sorriso Valvo, M., Reali, C., and Osso, I. (1978). "Digital terrain analysis for land evaluation". Geologia Applicata e Idrogeologia, 13, 69-127.

Carrara, A.E., Pugliese-Carratelli, and Merenda, L. (1977). "Computer-based data bank and statistical analysis of slope instability phenomenon". Zeitschrift für Geomorphologie, 21, 187-222.

Census. (2011). Ministry of Home Affairs, Govt. of India. Website: http://www.censusindia.gov.in/2011-common/census_2011.html.

Chandel, V.B.S., Brar, K.K., and Chauhan, Y. (2011). "RS- and GIS-based landslide hazard zonation of mountainous terrains: a study from Middle Himalayan Kullu District, Himachal". International Journal of Geomatics and Geosciences-Pradesh, India, 2, 121-132.

Choubey, V.D., and Litoria, P.K. (1990). "Terrain classification and land hazard mapping in KaLHI-Chakrata area (Garhwal Himalaya), India". ITC Journal, 1, 65-68.

Choubey, V.M., Mukherjee, P.K., Bajwa, B.S., and Walia, V. (2007). "Geological and tectonic influence on water–soil–radon relationship in Mandi–Manali area, Himachal Himalaya". Environmental Geology, 52, 1163-1171.

Cruden, D. (1991). "A simple definition of a landslide". Bull. Int. Assoc. Eng. Geology, 43, 27-29. Doi: .1007/BF02590167.

Dai, F.C., and Lee, C.F. (2002). "Landslide characteristics and slope instability modelling using GIS, Lantau Island, Hong Kong". Geomorphology, 42, 213-238.

Fawcett, T. (2006). "An introduction to ROC analysis". Pattern Recognition Letters, 27, 861-874.

Feizizadeh, B., and Blaschke, T. (2013). "IS-multicriteria decision analysis for landslide susceptibility mapping: comparing three methods for the Urmia Lake basin, Iran". Nat. Haz., 65, 2105-2128.

Gardner, J. S. (2002). "Natural hazard risk in the Lahaul District, Himachal Pradesh, India". Geographical Review, 92 (2), 282-306.

Gupta, R.P., and Joshi, B.C. (1990). "Landslide hazard zonation using the GIS approach- a case study from the Ramganga Catchment, Himalayas". Engineering Geology, 28, 119-131.

Guzzetti, F., Cardinali, M., and Reichenbach, P. (1996). "The influence of structural setting and lithology on landslide type and pattern". Environmental and Engineering Geoscience, 2 (4), 531-555.

Guzzetti, F., Galli, M., Reichebach, P., Ardizzone, F., and Cardinali, M. (2006). "Landslide hazard assessment in the Collazzone area, Umbria, Central Italy". Nat. Haz. Earth Syst. Sci., 6, 115-131.

Guzetti, F., Mondini, A.C., Cardinali, M., Fiorucci, F., Santangelo, M., and Chang, K-T. (2012). "Landslide inventory maps: new tools for an old problem". Earth Sci. Rev., 112, 42-66.

Hosmer, D.W., and Lameshow, S. (2000). "Applied logistic regression". 2nd Edn., John Wiley and Sons, London.

Kayastha, S.L. (1964). "The Himalayan Beas basin: a study in habitat, economy and society". Varanasi: Banaras Hindu University Press.

Lin, M.L., and Tung, C.C. (2003). "A GIS-based potential analysis of the landslides induced by the Chi-Chi Earthquake". Engineering Geology, 71, 63-77.

Mathew, J., Jha, V.K., and Rawat, G.S. (2007). "Weights of evidence modelling for landslide hazard zonation mapping in part of Bhagirathi valley, Uttarakhand". Current Science, 92 (5), 628-638.

Nandi, A., and Shakoor, A. (2009). "A GIS-based landslide susceptibility evaluation using bivariate and multivariate statistical analyses". Eng. Geol., 110 (1-2), 11-20.

Parker, R.N., Densmore, A.L., Rosser, N.J., de Michele, M., Li, Y., Huang, R., Whadcoat, S., and Petley, D.N. (2011). "Mass wasting triggered by the 2008 Wenchuan earthquake is greater than orogenic growth". Nature Geoscience, 4 (7), 449-452.

Phukon, P., Chetia, D., and Das, P. (2012). "Landslide susceptibility assessment in the Guwahati city, Assam using analytic hierarchy process [AHP] and geographic information system (GIS)". International Journal of Computer Applications in Engineering Sciences, 2 (1), 1-6.

Pourghasemi, H.R., Pardhasn, B., Gockeoghu, C., and Deylami Moezzi, K.D. (2012). "Landslide susceptibility mapping using a spatial multi-criteria evaluation model at Haraz watershed, Iran". Springer Verlag Berlin-Heidelberg, 23-49.

Rautela, P., and Thakur, V.C. (1999). "Landslide hazard zonation in Kaliganga and Madhyamahshwar valleys of Garhwal Himalaya: a GIS-based approach". Himalayan Geology, 20 (2), 31-44.

Richards, J.A., and Jia, X. (1999). "Remote sensing digital image analysis: an introduction". 3rd Edition, Springer Verlag, Heidelberg, Germany.

Saaty, T.L. (1980). "The analytic hierarchy process". New York: McGraw Hill International, Translated to Russian, Portuguese and Chinese, Revised Editions, Paperback (1996, 2000), Pittsburgh: RWS Publications.

Saaty, T.L. (2005). "Theory and applications of the analytic network process". Pittsburgh, PA: RWS Publications.

Sah, M.P., and Mazari, R.K. (2007). "An overview of the geoenvironmental status of the Lahaul Valley, Himachal Pradesh, India". Journal of Mountain Science, 4 (1), 3-23.

Saha, A. K., Gupta, R. P., Sarkar, I., Arora, M.K., and Csaplovics, E. (2005). "An approach for GIS-based statistical landslide susceptibility zonation with a case study in the Himalayas". Landslides, 2, 61-69.

Sarkar, S., Kanungo, D.P., and Mehrotra, G.S. (1995). "Landslide hazard zonation: a case study in Garhwal Himalaya, India". Mountain Research and Development, 15 (4), 301-309.

Sarkar, S., Roy, A.K., and Martha, T.R. (2013). "Landslide susceptibility assessment using information value method in parts of the Darjeeling Himalayas". Journal of Geological Society of India, October, 351-362.

Sharma, M., and Kumar, R. (2008). "GIS-based landslide hazard zonation: a case study on the Parwanoo area, Lesser and Outer Himalaya, H.P., India". Bulletin of Engineering Geology and the Environment, 67, 129-137.

Soeters, R., and van Westen, C.J. (1996). "Slope instability recognition: analysis and zonation". In: Turner, K.T., and Schuster, R.L. (eds.). Landslides: Investigation and Mitigation. Special Report No. 247, 129-177, Transportation Research Board, National Research Council, Washington, DC.

Trigila, A., Iadanza, C., and Spizzichino, D. (2010). "Quality assessment of the Italian landslide inventory using GIS processing". Landslides, 7, 455-470.

Van Westen, C.J. (1997). "Statistical landslide hazard analysis". In: van Westen, C.J. (Ed.), ILWIS 2.1 for Windows Application Guide. ITC Publication, Enschede, 73-84.

van Westen, C.J., Rengers, N., Terlien, M.T.J., and Soeters, R. (1997). "Prediction of the occurrence of slope instability phenomena through GIS-based hazard zonation". Geol. Rundsch., 86, 404-414.

van Westen, C.J. (2000). "The modelling of landslide hazards using GIS". Geophysics, 21, 241-255.

Xin, K.L., and Yan, T.Z. (1988). "Statistical prediction model for slope instability of metamorphosed rocks". In: Bonnard, C. (Ed.). Proceedings of the 5th International Symposium on Landslides, 2, 1269-1272. Lausanne, Balkema, Rotterdam.